Modeling Fire-Related Smoke Inhalation Injury Using the Human Lung-on-a-Chip and Organoid Platform: Pathogenesis Insights and Therapeutic Evaluation

Junmin Li[1], Dezhong Zhang[2], Yan Meng[1], Yongqing Chang[1], Wenbo Wei[3], Peng Wu[4], Lin Peng[4], Wei Chang[5], Wei Wang[5], Jie Huang[5], Jingjing Fang[6], Keming Zhu[1], and wan xiaojian[1]

[1]Changhai Hospital
[2]Huizhou Central People's Hospital
[3]Shenzhen People's Hospital
[4]Second Military Medical University First Hospital: Changhai Hospital
[5]Fudan University Shanghai Xuhui Central Hospital
[6]Naval Medical University

November 07, 2024

Abstract

Fire-related smoke inhalation-induced acute lung injury (SI-ALI) is a prevalent condition in modern fires, characterized by high mortality and a lack of targeted therapeutic options. Previous research has been hindered by instability in smoke generation and modeling methods, limiting the investigation of SI-ALI mechanisms. This study, for the first time, utilized organ-on-a-chip and organoid technologies, optimizing chip design and precisely controlling smoke generation from non-metallic materials to establish a human-relevant, physiologically accurate model of fire-related SI-ALI. The results demonstrate that this model effectively simulates the alveolar-capillary barrier and replicates key pathological features of lung injury, including oxidative stress, apoptosis, immune cell adhesion, inflammatory responses, capillary leakage, and mitochondrial damage. Injury responses of endothelial and epithelial cells to smoke exposure were thoroughly assessed at the organ level. Integrating proteomics and molecular biology techniques, along with comparisons to animal models, identified disease-specific pathways related to the spliceosome and carbon metabolism, as well as pathogenic molecules such as catechol-O-methyltransferase (COMT) and nitrilase 1 (NIT1). Furthermore, molecular docking of COMT revealed potential therapeutic candidates from the FDA-approved drug library, including Ractopamine HCl and Bimatoprost. The efficacy of intravenous vitamin C combined with nebulized budesonide was validated on the chip model, establishing a foundation for clinical applications. This study provides a robust model for investigating fire-related SI-ALI and offers novel insights into underlying mechanisms and therapeutic development.

Modeling Fire-Related Smoke Inhalation Injury Using the Human Lung-on-a-Chip and Organoid Platform: Pathogenesis Insights and Therapeutic Evaluation

Junmin Li[a,b,h,i,1], Dezhong Zhang[d,1], Yan Meng[a,b,h,i,1], Yongqing Chang[a,b,h,i,1],Wenbo Wei[e], Peng Wu[a,b,h,i], Lin Peng[a,b,h,i], Wei Chang[f], Wei Wang[f], Jie Huang[g], Jingjing Fang[c,*], Keming Zhu[a,b,h,i,*], Xiaojian Wan[a,b,h,i,*]

1. Department of Critical Care Medicine, Changhai Hospital, the Naval Medical University, Shanghai, 200433, China.
2. Intensive Care Medical Center, Changhai Hospital, the Naval Medical University, Shanghai, 200433, China.

3. Naval Medical Center, the Naval Medical University, Shanghai, 200433, China.
4. Huizhou First Maternal and Child Health Care Hospital, Guangdong, Huizhou, 516007, China.
5. The First Affiliated Hospital of Shenzhen University, Shenzhen Second People's Hospital, Shenzhen 518035, China.
6. Department of Emergency, Xuhui Hospital Affiliated to Fudan University, Shanghai, 200030, China.
7. Department of Respiratory and Critical Care Medicine, Xuhui Hospital Affiliated to Fudan University, Shanghai, 200030, China.
8. Department of Tropical Medicine, Changhai Hospital, the Naval Medical University, Shanghai, 200433, China.
9. Department of Maritime Clinical Medicine, Changhai Hospital, the Naval Medical University, Shanghai, 200433, China.

*Corresponding author.

Email addresses: Changhai168996@163.com (X. Wan), kmzhu@aliyun.com (K. Zhu), jjfang@smmu.edu.cn (J. Fang).

[1] These authors contributed equally in this work.

Abstract

Fire-related smoke inhalation-induced acute lung injury (SI-ALI) is a prevalent condition in modern fires, characterized by high mortality and a lack of targeted therapeutic options. Previous research has been hindered by instability in smoke generation and modeling methods, limiting the investigation of SI-ALI mechanisms. This study, for the first time, utilized organ-on-a-chip and organoid technologies, optimizing chip design and precisely controlling smoke generation from non-metallic materials to establish a human-relevant, physiologically accurate model of fire-related SI-ALI. The results demonstrate that this model effectively simulates the alveolar-capillary barrier and replicates key pathological features of lung injury, including oxidative stress, apoptosis, immune cell adhesion, inflammatory responses, capillary leakage, and mitochondrial damage. Injury responses of endothelial and epithelial cells to smoke exposure were thoroughly assessed at the organ level. Integrating proteomics and molecular biology techniques, along with comparisons to animal models, identified disease-specific pathways related to the spliceosome and carbon metabolism, as well as pathogenic molecules such as catechol-O-methyltransferase (COMT) and nitrilase 1 (NIT1). Furthermore, molecular docking of COMT revealed potential therapeutic candidates from the FDA-approved drug library, including Ractopamine HCl and Bimatoprost. The efficacy of intravenous vitamin C combined with nebulized budesonide was validated on the chip model, establishing a foundation for clinical applications. This study provides a robust model for investigating fire-related SI-ALI and offers novel insights into underlying mechanisms and therapeutic development.

Keywords : Organ-on-a-Chip; Organoids; Acute Lung Injury; Fire Incidents; Molecular Docking; Drug Screening

Introduction

Fire-related smoke inhalation-induced acute lung injury (SI-ALI) is among the most prevalent clinical injuries. The combustion of non-metallic materials indoors during a fire releases significant amounts of toxic substances, which can cause severe damage to the respiratory tract. In extreme cases, this can progress to acute respiratory distress syndrome (ARDS) or even multiple organ dysfunction syndrome (MODS)[1]. Studies have shown that burn patients with concurrent inhalation lung injury have a 40% higher mortality rate[2].

Unlike other forms of SI-ALI, such as those induced by cigarette smoke, wood burning, or exposure to single toxic gases[3, 4], fire-related SI-ALI is considerably more complex, especially in the modern era, due to the new composite materials used in modern wood manufacturing. Traditional wood, once the primary material for indoor furnishings, has largely been replaced by synthetic rubbers, resins, and other high-molecular-weight non-metallic materials. The combustion of these mixed materials during a fire releases large quantities of

toxic gases, including hydrogen cyanide (HCN), carbon monoxide (CO), and benzene[5]. These toxic gases, along with hazardous particulates, enter the respiratory system, triggering a cascade of pathological events such as oxidative stress, immune cell infiltration, inflammatory responses, and disruption of the alveolar-vascular barrier[6]. Unfortunately, no targeted therapies are currently available for fire-related SI-ALI, with treatment primarily relying on mechanical ventilation and supportive care. An appropriate model is essential for investigating the mechanisms of fire-related SI-ALI and developing effective therapeutics.

However, current models of fire-related SI-ALI face two significant challenges: the inhomogeneity of smoke generation and the inherent limitations of traditional animal and cell models. First, the composition and concentration of smoke can vary greatly depending on fire conditions, such as temperature and material composition[7], leading to the lack of reproducibility in these models. Moreover, traditional animal models, although commonly employed to investigate the mechanisms and replicate the pathological processes of SI-ALI[8, 9], are inherently limited due to physiological and genetic differences between animals and humans. These models are further constrained by ethical considerations, adherence to the 3R principles (Reduction, Replacement, Refinement), and the high costs and time demands associated with their use. Additionally, understanding the complex interactions between different cell types and elucidating their specific roles in SI-ALI is challenging in these models.

On the other hand, single-cell line models, frequently used in toxicity screening and mechanistic studies, also fail to accurately represent the complexity of SI-ALI[10, 11]. The lung comprises a diverse array of cell types—including epithelial, vascular, stromal and immune cells—that interact in complex pathophysiological processes. Furthermore, exposing lung epithelial cells to smoke extract in liquid form does not adequately simulate actual smoke exposure, as certain hydrophobic components of smoke are insoluble. Therefore, there is an urgent need to develop a stable, reproducible, human-derived model that is versatile and physiologically relevant, capable of faithfully replicating the pathological processes of fire-related SI-ALI.

Organ-on-a-chip technology offers a promising solution to the limitations inherent in traditional models[12]. Microengineered breathing lung chips have been developed to simulate human airway responses to cigarette smoke, particularly within the context of chronic obstructive pulmonary disease (COPD)[13]. These lung-on-chips (LOCs) have also been employed to study the nanotoxicity of TiO2 and ZnO nanoparticles on lung epithelial and endothelial cells, demonstrating the cytotoxicity, reactive oxygen species (ROS) production, and apoptosis induced by these nanoparticles[14]. Advanced LOCs serve as highly efficient platforms for drug screening, enabling the use of techniques such as transcriptomics, proteomics, and computational molecular biology to investigate disease pathology and facilitate drug development[15]. Additionally, lung organoids, which retain the unique cellular components and genetic characteristics of lung tissue, allow for the creation of more physiologically relevant disease models, thereby improving the accuracy of drug screening[16]. The integration of lung-on-a-chip and organoid technologies holds significant potential for simulating the pathological processes of fire-related SI-ALI, elucidating underlying mechanisms, and identifying effective treatments.

This study pioneers the integration of organ-on-a-chip and organoid technologies, enhancing the organ-on-a-chip system based on previous research. Materials were carefully blended to reflect the proportions of non-metallic components typically found in modern yachts, with precise control over the combustion process. The composition and concentration of smoke were monitored in real-time using Fourier-transform infrared spectroscopy (FTIR), effectively simulating the smoke production process during actual fires. Building on this foundation, a lung-on-a-chip model for fire-related SI-ALI was developed, successfully replicating key pathological processes in vitro and examining the responses of various cell types to smoke-induced damage. The study, combined with animal models, molecular biology techniques, proteomics, and molecular docking, explored the unique pathogenic mechanisms of fire-related SI-ALI and identified potential therapeutic drugs. Furthermore, the chip platform was utilized to evaluate the therapeutic potential of nebulized budesonide combined with intravenous vitamin C, with these findings validated in the organoid chip model. This research establishes a new paradigm for studying fire-related SI-ALI, providing valuable insights into its pathology and potential treatments.

Materials and methods

2.1 Design and fabrication of lung on-a-chip device

The LOC device comprises three layers. The upper and lower layers, fabricated from polydimethylsiloxane (PDMS), each contain three chambers. The upper layer features three rectangular chambers (10 mm long × 5 mm wide × 100 μm height) connected by channels 3 mm wide. The lower layer includes three independent rectangular chambers (15 mm long × 8 mm wide×100 μm height) that partially overlap with those of the upper layer, allowing observation of cells adhering to the base. A 25 μm-thick porous polyethylene terephthalate (PET) membrane with 8 μm pores separates these layers, which is treated with Aminopropyltriethoxysilane (APTES) for enhanced bonding. The PDMS mixture, with a 10:1 base-to-curing agent ratio by weight, is cast into a mold and cured at 65°C for 2 hours. Afterward, the PDMS layers are punched out and all three layers are plasma-treated before being bonded together. Based on previous literature[59, 60], hydrostatic pressure was utilized to provide fluid dynamics to the upper chamber of the chip, specifically through a pump-free system tilted at a 20-degree angle with a cycle frequency of 5 seconds. The variation in liquid height from an external reservoir generates fluid dynamics in the upper channel of the chip, effectively simulating blood flow.

2.2 Combustion materials and smoke generation system

Combustion utilizes non-metallic substances such as polyimide foam, rubber, sound insulation pads, acrylic paint, floor adhesive, nitrile rubber, and modified ethylene resin. These components are proportioned for a standard cruise ship room volume of 60 m^3. To ensure consistent combustion and smoke generation, materials are pulverized into fine particles (50-300 mesh) using a solid sample crusher and thoroughly mixed. This preparation seeks to minimize the variability in the smoke produced during combustion.

The combustion control system (HOPE-MED 8054F, designed and manufactured by Tianjin Heping Manufacturing Co., Ltd., Tianjin, China), was deployed in this study. The prepared materials were placed in a tube furnace and heated at a rate of 20°C/min until the target temperature of 600°C was achieved. Smoke generation began at 300°C. Thereafter, the circulation pump was activated, introducing combustion gas into the toxic chamber. The smoke generated by the HOPE-MED 8054F during the first 20 minutes was collected in a Tedlar® Gas Sampling Bag (Sigma-Aldrich, USA) for use in the subsequent modeling of acute lung injury in an organ-on-chip system.

A portable Fourier Transform Infrared Spectrometer (FTIR) (Gasmet DX-4020) was used to analyze smoke composition in real-time during combustion. The FTIR analyzer was preconditioned for 10 minutes. Pure nitrogen gas was used to calibrate the gas chamber as the background. Within the spectral range of 4000-400 cm^{-1}, 50 gas components were identified for rapid quantification of the gases emitted during combustion. Sampling analysis was performed at one-minute intervals until combustion ceased.

2.3 Cell culture on the LOC device and modeling the SI-ALI on the chip

Lung epithelial cells (purchased from ATCC, CCL-185) were propagated in Dulbecco's Modified Eagle's Medium (DMEM, OPM Biosciences, China) supplemented with 10% fetal bovine serum (FBS) and 1% penicillin-streptomycin. Human umbilical vein endothelial cells (HUVEC, purchased from ATCC, CRL-1730) were cultured in endothelial cell medium (ECM, ScienCell, USA). Human myeloid leukemia mononuclear cells (THP-1, purchased from ATCC, TIB-202) were cultured in RPMI 1640 medium (OPM Biosciences, China) containing 10% FBS, 0.05mM β-Mercaptoethano, and 1% penicillin-streptomycin. Prior to cell seeding, the LOC devices were sterilized by UV irradiation, and the porous membranes were preconditioned with collagen I (200 ug/mL, Suzhou Jiyan Biotech. Co. Ltd., China) at 37°C overnight. All cells incubated at 37°C in a 95% humidified atmosphere with 5% CO_2. For seeding on the lung on-a-chip, approximately 10ˆ5 epithelial cells were introduced onto the membrane in the lower chambers and the device was inverted for four hours to facilitate cell attachment. Subsequently, the device was reoriented, and ˜5 × 10ˆ5 HUVECs were seeded in the top channels. After 24 hours, the chip was integrated with the dynamic system, set at a 20° incline and rotating at a frequency of 5 seconds per cycle. THP-1 cells (treated with 200nM PMA for 3 days initially,

and then cultured for an additional 5 days in fresh RPMI 1640 medium[17]) were seeded in the top channels prior to smoke exposure. To visualize the alveolar-capillary barrier, HUVECs were labeled with PKH26 and epithelial cells with PKH67 (both from Sigma-Aldrich, USA), following the manufacturers' instructions. Confocal laser scanning microscopy (Leica, Germany) was utilized to assess the barrier. To simulate SI-ALI, smoke was drawn from the gas sampling bag using a 20 ml syringe and delivered into each lower chamber of the chip at an approximate rate of 0.6 ml/h for 60 minutes via a micro push pump. It is important to note that, at the start of the model setup, approximately 0.5 ml of smoke was rapidly injected within 1 minute to ensure uniform smoke concentration and exposure duration across all alveolar chambers.

Lung organoids were derived from non-cancerous distal tissues of patient undergoing lung cancer resection. Utilization of human samples was authorized by the Ethics Committee of Shanghai Xuhui Central Hospital (SOP-IEC-033-AF02), with written informed consent from all subjects. The procedure for isolating and culturing lung organoids was carried out as detailed in the provided manual (OCK-010, Suzhou Jiyan Biotech Co., Ltd., China; further information can be found at http://dubbbbrv.s10.myxypt.com/product/817.html). Specifically, within six hours of tissue sampling, terminal tissue from a non-cancerous region was selected and subjected to enzymatic digestion. Following complete digestion, fully dissociated cell clusters were isolated via differential centrifugation, with larger, undigested tissue fragments removed. Red blood cell lysis was then performed. The resulting cell clusters were mixed with Matrigel, combined with pre-warmed complete culture medium, and incubated at 37°C in a 95% humidified atmosphere with 5% CO_2. As organoids proliferate and increase in size, central regions are prone to apoptosis and necrosis, requiring timely passaging. Typically, primary organoids are passaged after 7-15 days, with subsequent generations passaged every 5-7 days.

To establish the alveolar-capillary barrier, single cells from lung epithelial organoids were combined with 10% Matrigel in complete medium (OCM-010, Suzhou Jiyan Biotech. Co. Ltd., China), followed by being seeded and cultured on the bottom surface of membrane in the chip for 48 hours. The HUVECs were cultured on the top surface of membrane for 24 hours after the epithelial cells adhered on the bottom of membrane. The dynamic culture were manipulated after both cells reached above 90% confluency. The smoke stimulation was same as above procedure.

2.4 Modeling SI-ALI in vivo based on animal model

Male C57/Bl6 mice, aged 6-8 weeks, were obtained from the Naval Medical University, People's Liberation Army, and housed in compliance with applicable ethical standards. The SI-ALI model was induced using the HOPE-MED 8054F system to generate smoke from combusted non-metallic materials, proportionally blended and pulverized. Upon the combustion furnace's stabilization at 600°C, the animals were subjected to the smoke for 20 minutes to evoke acute lung injury. Lung tissues were harvested 6 hours post-exposure for further analysis.

2.5 Histopathological analysis and lung injury scoring

Mouse lung samples were fixed in a 4% paraformaldehyde solution, followed by dehydration and embedding in paraffin. The samples were then sectioned into 5 μm thick slices. These sections were then stained with hematoxylin and eosin (H&E) for microscopic evaluation of morphological alterations of lung tissues and lung injury severity was quantified using a scoring system. This system rated alveolar edema, congestion, inflammatory infiltration, and interstitial thickening on a scale from 0 (normal) to 4 (diffuse involvement), with increasing scores denoting escalating lesion area within the field of view. The aggregated scores from these categories facilitated comparative analysis between groups.

2.7 Immunostaining and multiplex immunohistochemistry (mIHC)

Cells in the LOC channels were fixed with 4% paraformaldehyde (PFA) for 20 minutes at room temperature (RT) after rinsing with PBS. They were then permeabilized with 0.2% Triton-X for 15 minutes and blocked with 5% bovine serum albumin (BSA) for 1 hour at RT. Subsequently, the samples were incubated overnight at 4°C with primary antibodies: CD31 (diluted 1:400, cat no. 281583, Abcam, Cambridge, MA, USA) and E-cadherin (diluted 1:200, cat no. 231303, Abcam). After three washes with PBS, fluorescently labeled

secondary antibodies were applied for 1 hour at room temperature: donkey anti-rabbit IgG H&L (Alexa Fluor® 647) (diluted 1/200, cat no. ab150075, Abcam) and Goat Anti-Mouse IgG H&L (Alexa Fluor® 488) (2ug/ml, cat no. ab150117, Abcam). Following additional washes, cells were stained with DAPI for 5 minutes. The membranes containing the cells were then removed from the chip and mounted on cover glass for confocal microscopy imaging.

As for the method of multiplex immunohistochemistry (mIHC), the lung organoid derived epithelial cells on the chip were fixed in 4% PFA for 20 min at RT. The lung organoids were fixed with 4% PFA for 2h at RT after discarding Matrigel. Then, they were mixed with a special embedding gel (SEgel, Suzhou Jiyan Biotech. Co. Ltd., China) for 30 min at 37°C for solidification. These organoids in the SEgel were further fixed with 4% PFA overnight at RT, followed by gradient dehydration with 20%, 30%, and 40% sucrose. After dehydration, they were embedded in optimal cutting temperature compound (OCT, Japan) for frozen sectioning. The chip sample and organoid slides were treated by antigen retrieval through microwave treatment. Endogenous peroxidase activity was quenched, and the samples were then blocked with 5% BSA for 30 minutes. Subsequently, the samples were incubated with primary antibodies overnight at 4°C. After three washes with 1X PBS buffer, the samples were incubated with horseradish peroxidase (HRP)-conjugated secondary antibodies for 50 minutes at RT. Following a quick wash in 1X PBS buffer, an appropriate fluorophore-conjugated tyramide signal amplification (TSA) was applied for 10 minutes at RT. Microwave treatment was performed to strip the tissue-bound primary/secondary antibody complexes, preparing the samples for labeling with the next marker. This process was repeated for primary antibodies (SFTPC, 1:800, cat no. GB114059, Servicebio; E-cadherin, 1:400, cat no. 3195S, CST), HRP-conjugated secondary antibodies (cat no. WAS1201100, World Advanced Science Co., Ltd., China), and fluorophore-conjugated TSA (TSA570, WAS1003050; TSA520, WAS1002050) until all markers were labeled. Finally, the samples were stained with DAPI in the dark for 10 minutes at RT and mounted with an anti-fade mounting medium. The images were captured using the PANNORAMIC MIDI II imaging system. The lung organoid epithelial cells on the chip were imaged with confocal microscopy (Leica, Germany).

2.8 Enzyme-linked immunosorbent assays (ELISA)

To evaluate the secretion of IL-6, TNF-α and IL-1β from the vascular layer of the chip, culture medium was harvested from the top layer, centrifuged at 12,000 rpm for 10 minutes at 4°C, and the supernatant collected. The quantification of IL-6, TNF-α, and IL-1β was carried out using human ELISA kits (Biolegend, USA) according to the manufacturer's instructions.

2.9 Quantitative PCR (qPCR)

Total RNA was extracted from the top and bottom layers of the chip using an RNA extraction kit (cat no. AG21023, Accurate bio, China) and subsequently converted to cDNA using a reverse transcription kit (cat no. AG11707, Accurate bio, China), with inputs ranging from 50 to 500 ng of RNA. The expression levels of inflammatory cytokines and other genes were assessed by fluorescence-based qPCR. Primers information was provided in Table 1. PCR amplification involved an initial step of 50°C for 10 minutes, denaturation at 95°C for 1 minute, followed by 45 cycles of 95°C for 15 seconds, and 60°C for 45 seconds. Expression data were quantified employing the 2-[?][?]Ct method.

2.10 Analysis of THP-1 adhesion on the endothelium in the lung chip

THP-1 cell adhesion on the endothelium within the lung chip was evaluated by pre-treating the cells with a live/dead staining reagent (Thermo, USA). Following this, THP-1 cells were introduced to the upper layer of the chip. Four hours post-smoke exposure, THP-1 cell aggregation in both control and experimental group (mostly stained in green) using fluorescence microscope. Image quantification was executed using ImageJ software.

2.11 Permeability monitoring of alveolar-capillary barrier on the chip

The permeability of the alveolar-capillary barrier on the chip was assessed by measuring the diffusion rate of FITC-dextran (40 kDa, purchased from Thermo, USA) from the upper vascular layer to the lower alveolar

compartment. Following smoke exposure, media with FITC-dextran were added to the upper channels. Samples from the lower chambers were collected at set intervals (0 and 60 min), and their fluorescence intensities were measured with a plate reader. This rate was computed to ascertain barrier permeability. Real-time observation of fluorescence in the lower layer was also performed to assess permeability through the chip's transparent sections.

2.12 Proteomics analysis

Lung tissues from mice and cells from the chips were harvested for proteomic studies. Tissues and cells were lysed with SDT buffer and sonicated intermittently (10 seconds on, 10 seconds off) for a total of 2 minutes to enhance disruption. Centrifugation at 12,000 rpm for 10 minutes ensued to discard insoluble fragments. Proteins were extracted and subsequently digested using the filter-aided sample preparation (FASP) method. Protein alkylation was accomplished using IAA, followed by trypsin digestion to generate peptide fragments. Following peptide desalting, data acquisition was conducted using an LC-MS/MS system consisting of Thermo Fisher's Easy-nano LC and QE Plus instruments.

2.13 TUNEL and ROS assays

Apoptotic cells were identified via TUNEL using a One Step TUNEL Apoptosis Assay Kit (C1088, Beyotime, China), while ROS detection was performed using the Reactive Oxygen Species Assay Kit (S0033M, Beyotime, China). Detailed protocols for these assays can be found in the manufacturer's instruction manual. Following the aforementioned procedures, the samples were observed under a fluorescence microscope and images were captured. Subsequently, the obtained images were quantified using image analysis software, specifically ImageJ.

$$\mathbf{TEER} = (\mathbf{R} - \mathbf{R_0}) \times \mathbf{S}$$

R: Resistance value of the experimental group.

$\mathbf{R_0}$: Resistance value of blank group (without cell).

S: Area.

2.15 The calculation of the smoke flow rate of each lower chamber of the chip

$$V_{chip} = \frac{V_{human} \times S_{chip}}{S_{human}}$$

$V_{\mathbf{chip}}$: The flow rate of each lower chamber in chip.

$V_{\mathbf{human}}$: Minute ventilation of human, set at about 7L/min.

$S_{\mathbf{chip}}$: The area of per lower chamber in chip, set at approximately 1cm^2.

$S_{\mathbf{human}}$: The area of alveolar surface of human, set at around 70m^2.

2.16 Transmission electron microscope (TEM)

The central membrane of the chip was isolated and fixed in 2.5% glutaraldehyde for 2 hours at 4. Then, we followed previously reported methods and obtained samples for TEM. The morphology of organelles in the samples was characterized using a JEM 1400 transmission electron microscope (JEOL, Tokyo, Japan).

2.17 Molecular Docking

The protein structures of interest were retrieved and downloaded from the Protein Data Bank (PDB) website. For proteins without reported structures, the three-dimensional structures were predicted using AlphaFold2. Subsequently, docking grid files were generated using the Glide Grid module of Schrödinger, which facilitated the molecular docking studies. A drug library was downloaded from the FDA (Selleckchem.com) and processed using Schrödinger's LigPrep module. This processing included protonation, desalting, hydrogenation, generation of tautomers and stereoisomers, and energy minimization. The virtual screening process began with an initial round of high-throughput virtual screening (HTVS) using Schrödinger's Glide module. In this stage, the top 10% of molecules based on their scores were retained for further analysis. These molecules were then subjected to standard precision (SP) screening. The top 10% of molecules from the SP screening were further refined through extra precision (XP) screening.

2.18 Detection of SOD, MDA, and GSH

The activities of superoxide dismutase (SOD) and the levels of glutathione (GSH) and malondialdehyde (MDA) in lung tissues were quantified using a commercial assay kit(Nanjing Jiancheng Bio Co., Ltd., China). The measurements were conducted following the protocols provided by the manufacturer.

2.19 Statistical analysis

Data were compiled in Microsoft Excel, with statistical graphics created in GraphPad Prism (9.5.0). Comparisons between two groups were made using Student's t-test, while one-way ANOVA, accompanied by post hoc tests, was utilized for multiple group comparisons. Results were displayed as bar graphs with error bars representing mean ± SD. Results were considered significantly different when P <0.05, with values at *P <0.05, **P <0.01, ***P <0.001, and ****P <0.0001.

Results

3.1 Mimicking the alveolar-capillary barrier based on LOC

The schematic for this study is shown in Figure 1, which includes a diagram of lung injury, the LOC system, and major experimental methods. The LOC device featured an upper layer for culturing human umbilical vein endothelial cells (HUVECs), simulating blood vessels, and three independent lower chambers for culturing lung epithelial cells (Figure 2A-a, b, and Supplementary Figure 1). Elastic tubes interconnected multiple lung chips, facilitating communication between alveolar channels (Figure 2A-e). A gravity-driven flow strategy was employed using a programmable rocking device, ensuring stable fluid flow in the vascular channel by adjusting the angle and frequency (20° and 5 cycles per minute, respectively) (Figure 2A-c, d, and Videos 1-2).

HUVECs and lung epithelial cells, stained with live-cell dyes (red and green, respectively), were cultured on opposite sides of the membrane to establish the alveolar-capillary interface. On day 7, cell viability exceeded 90%, as shown by the live/dead staining assay (Supplementary Figure 1A). The resistance value reached a steady state from days 3 to 7, indicating the formation of a robust alveolar-capillary barrier (Supplementary Figure 1B). Immunofluorescence assays confirmed the expression of E-cadherin and CD31 in the epithelial cells and HUVECs, respectively (Supplementary Figure 1C).

3.2 Modeling and characterizing fire-related SI-ALI on the LOC

The combustion control system and non-metallic materials, including polyimide foam, rubber, sound insulation pads, acrylic paint, floor adhesive, nitrile rubber, and modified ethylene resin, are illustrated in Figures 2B-a and 2B-c. Combustion byproducts were monitored using a portable Fourier Transform Infrared Spectrometer (FTIR) (Figure 2B-b). To evaluate combustion stability, emissions of gases, including nitrous oxide (N2O), carbon monoxide (CO), styrene (C8H8), and hydrogen cyanide (HCN), were quantified. The results showed consistent trends in the concentration changes of these gases across different batches of material during combustion (Supplementary Figure 2C), with detailed compositions provided in Supplementary Text 1.

To replicate the SI-ALI process observed in vivo (Figures 1A and 3F), the collected smoke was introduced into the lower compartments of the lung chip using a syringe to simulate alveolar smoke exposure (Figure 2C). Oxidative stress and apoptosis assays demonstrated increased ROS production (Figure 3C) and elevated cell apoptosis (Figure 3A) following smoke exposure. Transmission electron microscopy (TEM) revealed significant damage to the mitochondria and endoplasmic reticulum (Figure 3E). Leakage assays detected the rapid translocation of macromolecular substances (FITC-dextran, 40 kDa) from the vascular to the alveolar channel under smoke exposure (Figure 3B), indicating a compromised alveolar-capillary barrier. Additionally, a marked increase in the adhesion of activated THP-1 cells to the barrier was observed in the smoke-exposed group compared to the control group (Figure 3D). Inflammation- and apoptosis-related genes, including IL-6, TNF-α, and caspase-3, were upregulated in both epithelial and endothelial cells (Figure 4A-b, c, e), while IL-1β and NF-ϰB were predominantly upregulated in epithelial cells alone (Figure 4A-a, f). Notably, IL-10 expression remained unchanged (Figure 4A-d). ELISA results further confirmed that smoke exposure stimulates the release of TNF-α, IL-6, and IL-1β, independent of THP-1 cell presence (Figure 4B). These findings underscore the detrimental impact of smoke on the alveolar-capillary barrier, including the induction of oxidative stress, cellular apoptosis, mitochondrial damage, and the initiation of an inflammatory cascade accompanied by enhanced inflammatory cell adhesion.

3.3 Proteomic profiling analysis of SI-ALI based on LOC

Proteomic analysis of the chip model identified 104 differentially expressed proteins (DEPs), with 85 upregulated and 19 downregulated. These DEPs were characterized by a fold change of [?] 0.83 or [?] 1.2 and a p-value of < 0.05 (Supplementary Text 2). Kyoto Encyclopedia of Genes and Genomes (KEGG) pathway analysis highlighted the enrichment of these proteins in several biological processes, including cysteine and methionine metabolism, amino acid biosynthesis, mineral absorption, carbon metabolism, and the functional roles of lysosomes and spliceosomes (Figure 5B and Supplementary Text 2). Gene Ontology Biological Processes (GOBP) analysis indicated involvement in lymphocyte aggregation, cellular response to erythropoietin, CAMKK-AMPK signaling cascade, mitochondrial protein processing, and DNA methylation maintenance. Gene Ontology Cellular Component (GOCC) terms were concentrated in clathrin-coated structures, the COPI vesicle coat, and components of the spliceosome. Gene Ontology Molecular Function (GOMF) analysis revealed associations with T cell receptor binding, G-protein subunit binding, and retromer complex binding (Figure 5A and Supplementary Text 2).

3.4 Proteomic profiling analysis of SI-ALI in in vivo model

The same smoke mixture was used to establish the SI-ALI model in C57 mice, enabling a comparative analysis of differences and similarities between the in vivo and lung chip models. The in vivo smoke-exposed group exhibited significantly elevated lung injury scores and wet/dry weight ratios compared to the control group (Supplementary Figures 2A and 2B-a). Additionally, oxidative stress-related and injury markers in the lungs, such as superoxide dismutase (SOD), lactate dehydrogenase (LDH), and glutathione (GSH), showed substantial alterations (Supplementary Figures 2B-b to 2B-d). Further proteomic analysis of lung tissue identified 566 differentially expressed proteins (DEPs), with 465 upregulated and 101 downregulated (fold change [?] 0.83 or [?] 1.2 and p-value < 0.05) (Supplementary Text 3). KEGG pathway analysis indicated that these DEPs were enriched in various biological processes, including metabolism, vesicular transport,

and tight junction integrity (Supplementary Text 3). Gene Ontology Biological Processes (GOBP) analysis revealed involvement in skeletal muscle satellite cell migration, regulation of mRNA stability in response to oxidative stress, and negative regulation of both ubiquitin-specific protease activity and nitrosative stress-induced apoptotic signaling. Gene Ontology Cellular Component (GOCC) terms were enriched in structures such as collagen type I trimer and mitochondrial complexes. Gene Ontology Molecular Function (GOMF) analysis identified significant enrichment in functions ranging from phosphoserine binding to various oxidoreductase activities (Supplementary Text 3). Overlap of KEGG pathways and GO terms between the animal and lung chip models is detailed in Supplementary Figure 3.

3.5 Verification of SI-ALI-associated genes in LOC and Molecular Docking of Key Molecules

Comparison of DEPs from the LOC and in vivo models identified six common genes: EPS15L1, CRIP1, SLC25A10, ATL3, SRP68, and Catechol-O-Methyltransferase (COMT), with only COMT being upregulated in both models (Figures 5C-D). We evaluated mRNA expression levels of COMT and other significantly altered DEPs in the chip model, including Dedicator of cytokinesis 2 (DOCK2), thiosulfate sulfurtransferase (TST), Keratinocyte Growth Factor Receptor-Related Protein 1 (KRR1), nitrilase-like protein 1 (NIT1), and RAP1 GTPase-GDP dissociation stimulator 1 (RAP1GDS1) (Figure 6A). The expression of COMT and DOCK2 was upregulated in both epithelial and endothelial cells in the smoke exposure group (Figures 6A-a, f), consistent with the proteomic findings. Moreover, mRNA expression levels of TST, NIT1, and RAP1GDS1 corresponded with the proteomic data (Figures 6A-b, d, e). Additionally, KRR1 showed upregulation in the epithelium following smoke exposure, with no significant change in the endothelium (Figure 6C-c). These results demonstrate that the identified molecules are consistent at both transcriptional and translational levels, except for KRR1.

To further explore therapeutic drugs, we employed computational biology to perform molecular docking of COMT with potential drugs. The results indicated that several FDA-approved drugs, including Ractopamine HCl, Bimatoprost, Ibutilide Fumarate, Fenoterol, Prucalopride Succinate, and Fenoterol hydrobromide, may have therapeutic effects (Figure 6B).

3.6 The effects of Budesonide nebulization combined with intravenous Vitamin C on the SI-ALI in vitro

We further employed the LOC as a platform to explore the therapeutic efficacy of budesonide nebulization in conjunction with intravenous Vitamin C for mitigating SI-ALI. This treatment regimen was based on clinical medication standards[18]. Following smoke exposure, 2.4 mg/ml Vitamin C was introduced into the upper chamber for 4 hours, while budesonide (diluted with normal saline at a 1:1 ratio) was administered into the lower chamber for 30 minutes. The results showed that the drug combination significantly reduced oxidative stress (Figure 7A). The mRNA expression of IL-1β, NF-κB, TNF-α, and IL-10 decreased in both epithelial and endothelial cells (Figures 7B-a, c, d, f). IL-6 expression decreased in the endothelium but showed no significant change in the epithelium (Figure 7B-b). The gene expression of caspase-3, a crucial apoptotic molecule, also decreased in both cell types within the treatment group (Figure 7B-e). These findings provide experimental evidence supporting the clinical application of budesonide nebulization combined with intravenous Vitamin C for reducing inflammation, oxidative stress, and apoptosis in fire-related SI-ALI.

3.7 Reproduction and verification of SI-ALI by human-derived lung organoid on chip

Acknowledging the distinct differences between cell lines and primary cells, we sought to validate our findings using human-derived lung organoids. Bright-field microscopy illustrated the development and characteristic self-organization of lung organoids (Figure 8A). Immunofluorescence staining confirmed their terminal differentiation into alveoli, identified by SFTPC and E-cadherin biomarkers (Figure 8B), without expression of the airway basal cell marker KRT5 (not shown). Subsequently, we incorporated lung-organoid-derived epithelial cells into the lung chip system. Immunofluorescence images revealed the morphological features of the epithelium on the chip (Figure 8C). These cells retained the expression of alveolar-specific markers (SFTPC and E-cadherin), resembling normal lung tissue to some extent.

We further validated the SI-ALI-related genes identified in the previous experiment. The mRNA expression levels of TST, NIT1, and RAP1GDS1 were reduced in both lung-organoid-derived epithelial cells and endothelial cells in the smoke-exposed group (Figures 8E-b, d, e). The mRNA expression of KRR1 increased in epithelial cells but decreased in endothelial cells in the smoke-exposed group (Figure 8E-b). The expression of COMT and DOCK2 tended to increase in both lung-organoid-derived epithelial cells and endothelial cells in the smoke-exposed group (Figures 8E-a, f), consistent with the proteomic findings from the chip model.

Upon administering the drug combination, qPCR analysis revealed varying degrees of reduction in the expression of inflammation-related genes (IL-1β, TNF-α, NF-ϰB, IL-6, and IL-10) across different cell components (Figures 8E-a, b, c, d, f). These results were consistent with findings from the cell line chip model. However, the expression of the apoptosis-related gene caspase-3 showed no significant change in the treated group of lung-organoid-derived epithelial cells (Figure 8E-e).

Discussion

This study marks the first application of organ-on-a-chip and organoid technologies to create a human-derived, more physiologically relevant, and functionally diverse model for fire-related smoke inhalation acute lung injury (SI-ALI). Through the integration of advanced methodologies, deeper insights into the pathophysiological mechanisms of fire-related SI-ALI have been achieved, along with the identification of potential therapeutic agents. This research provides a novel and robust platform for advancing both the study and treatment of fire-related SI-ALI.

Previous research on lung injury from fire-related smoke inhalation primarily used wood combustion smoke, which posed limitations due to the lack of control over combustion processes and unclear smoke concentrations, often relying on subjective estimates, thus compromising model stability[19]. Additionally, the composition of natural wood differs significantly from modern construction materials, making traditional data inadequate for contemporary fire-related SI-ALI studies[20]. By controlling material proportions and combustion processes, a system was developed to simulate modern non-metallic material combustion accurately (Figure 2B, Supplementary Figure 2C and Supplementary Text 1). Fourier-transform infrared spectroscopy confirmed the system's stability, providing a foundation for a reproducible SI-ALI model.

To create a more physiologically relevant SI-ALI model, organ-on-a-chip and organoid technologies were integrated. However, traditional lung chip models had limitations[21], such as complex perfusion pumps prone to bubble formation and contamination, as well as limited cell seeding capacity. To address these issues, an optimized lung chip model was developed with a gravity-driven, pump-less system to reduce contamination risks and improve practicality[22]. The expanded cell seeding area allowed for three parallel experiments within a single chip (details in the methodology section), increasing efficiency and enabling advanced molecular research. The chip design included a non-overlapping area between the vascular and alveolar layers, allowing real-time observation of capillary leakage and other pathological processes (Figures 1B and 2A).

A co-culture system of human alveolar epithelial and endothelial cells was established on the chip, simulating the alveolar-capillary barrier (Figure 3F). Over time, increased transepithelial resistance indicated tight junction formation (Supplementary Figure 1B). Confocal microscopy confirmed the bilayer structure, demonstrating successful barrier formation (Supplementary Figures 1C-D). This model allowed for the direct introduction of smoke into the alveolar chamber, simulating fire-related lung damage (Figure 2C). The chip technology bypassed the need for gases to dissolve in an aqueous solution, providing a more accurate replication of smoke damage to the alveolar epithelium and allowing for comprehensive analysis of intercellular interactions during injury[23].

The chip's response to prolonged toxic smoke exposure revealed oxidative stress and apoptosis, consistent with clinical findings[24-26]. Electron microscopy showed significant subcellular abnormalities, such as dense mitochondria and altered endoplasmic reticulum structures. Increased macrophage adhesion and chemotaxis were observed, aligning with clinical immune cell infiltration findings. The non-overlapping chip areas enabled real-time observation of alveolar-capillary leakage, challenging to replicate in traditional experiments. ELISA

analysis indicated a substantial release of inflammatory cytokines following smoke exposure, independent of immune cell presence (Figures 3 and 4).

The advanced chip design allowed for separate extraction of endothelial and epithelial cells for molecular analysis. Despite direct smoke stimulation of epithelial cells, qPCR analysis showed a similar response in endothelial cells, with upregulated inflammation and apoptosis-related genes, highlighting intercellular signaling during smoke exposure. This interaction, overlooked in previous single-cell models, warrants further investigation in fire-related SI-ALI (Figure 4).

To further elucidate the mechanisms of fire-related SI-ALI, a proteomic analysis was conducted to identify differentially expressed proteins (DEPs) post-smoke exposure in the chip model. KEGG enrichment analysis indicated these DEPs are involved in critical pathways such as cysteine and methionine metabolism, amino acid biosynthesis, mineral absorption, carbon metabolism, lysosomal function, and spliceosomal activity (Figure 5B and Supplementary Text 2). Notably, cysteine and methionine metabolism, linked to sepsis-related lung damage, and amino acid biosynthesis, associated with ferroptosis and drug efficacy in sepsis-induced lung injury, were emphasized[27, 28]. The role of mineral absorption, pertinent to injuries caused by particulate inhalation (e.g., graphene, asbestos), aligns with the smoke's solid particle composition[29, 30]. The enrichment of PSAT1 in carbon metabolism suggests novel research avenues for SI-ALI[31]. Autophagy's role, especially in lysosomal function, is highlighted in sepsis, COPD, and COVID-19 contexts[32-34], while the underexplored spliceosome's involvement is supported by its association with phosgene-induced lung injury[35], reinforcing the relevance of the identified pathways.

Gene Ontology Biological Process (GOBP) analysis revealed pathways including lymphocyte aggregation, CAMKK-AMPK signaling, mitochondrial protein processing, DNA methylation maintenance, and L-serine biosynthesis. Lymphocyte aggregation, linked to the inflammatory cascade in acute lung injury[36, 37]and CAMKK-AMPK signaling, associated with smoking-related lung cancer[38], were observed. Mitochondrial damage, linked to ferroptosis[39], aligns with the damage seen in smoke-exposed cells (Figure 3E), consistent with proteomic findings. The maintenance of DNA methylation is crucial for normal lung function, with its disruption noted in COPD[40]. Serine's role in nucleotide synthesis and antioxidant defense was noted[41, 42], while the hypermethylation of CpG islands, particularly the IFN-γ promoter via the PI3K-Akt-DNMT3b pathway, was linked to lung inflammation[43]. The depalmitoylation pathway remains underexplored in lung injury, but our analysis suggests its relevance, highlighting the complex pathology mirrored in clinical presentations.

To compare in vivo and chip models, a mouse model of fire-related SI-ALI was established. Histopathological analysis revealed significant lung damage (Supplementary Figure 2A and 2B), consistent with oxidative stress and cellular damage findings, aligning with the results of previous research[44, 45] and the chip model. Proteomic analysis showed more DEPs in the animal model, likely due to tissue complexity. However, both models shared enrichment in carbon metabolism and spliceosomal pathways, with common pathways including SRP-dependent co-translational protein targeting and small GTPase-mediated signaling, associated with metabolism, ROS, and apoptosis. The observed differences are attributed to species-specific variations but underscore the models' collective reflection of SI-ALI pathology, providing insights into underlying mechanisms (Supplementary Text 3).

Subsequent focus was on molecules with significant fold-change in the chip model, specifically DOCK2, TST, NIT1, RAP1GDS1, and KRR1. These molecules were investigated for endothelial and epithelial cell responses to smoke exposure (Figure 5D and Figure 6A). TST, involved in enhancing mitochondrial function and reducing ROS[46], and NIT1, responsible for hydrolyzing deaminated glutathione, have been underexplored in lung injury[47]. RAP1GDS1, linked to lung carcinogenesis[48, 49], and DOCK2, with anti-inflammatory properties, suggest potential as SI-ALI markers and therapeutic targets[50, 51]. These findings highlight critical molecules relevant to fire-related SI-ALI, warranting further investigation.

In the combined proteomic analysis of animal and chip models, only COMT consistently showed an upward expression trend, observed at both transcriptional and translational levels in endothelial and epithelial

cells (Figure 5C-D and Figure 6A). COMT, involved in catecholamine metabolism, may reduce oxidative stress from polycyclic aromatic hydrocarbons (PAHs) in A549 cells[52]and regulate lung water and sodium storage[53]. However, its role in smoke-induced acute lung injury (SI-ALI) remains largely unexplored. Our findings suggest that COMT could be crucial in the pathology of fire-related SI-ALI.

To identify potential therapies, a computational analysis of COMT's structure was performed[54]. Screening against the FDA-approved drug library revealed compounds like Ractopamine HCl, Bimatoprost, and Fenoterol Hydrobromide (Figure 6B and Supplementary Text 4). These drugs, targeting 5-HT, adrenergic, and prostaglandin receptors, are mainly used for glaucoma and respiratory conditions, yet their relevance to lung injury is unexamined. Our study indicates they may offer therapeutic potential in fire-related SI-ALI, although further validation is needed.

The chip model's drug screening ability was further explored for SI-ALI treatment development. Severe oxidative stress and inflammation following smoke exposure were consistent with clinical observations. To address these, intravenous vitamin C and nebulized budesonide were tested, significantly reducing oxidative stress and inflammation (Figure 7).

Vitamin C is known for its antioxidant and immune-modulating effects, with high doses shown to mitigate organ damage in sepsis[55], suggesting it may benefit SI-ALI treatment. However, the absence of clinical trials leaves no established guidelines. Glucocorticoids, despite their anti-inflammatory properties, pose risks like electrolyte imbalances and immunosuppression[56]. Budesonide, when nebulized, may minimize systemic side effects, offering potential for fire-related SI-ALI[57], though clinical evidence remains limited.

This study indicates that the combined therapy holds promise, providing a foundation for clinical use while underscoring the need for further research. The chip model's advanced features enabled evaluation of different administration routes, which traditional models struggle to achieve. This reinforces the chip's value in preclinical drug testing and new treatment development for SI-ALI.

Given the superior tissue specificity of human-derived lung organoids compared to cell lines[58], ethical approval was obtained to culture lung organoids (Figure 8A-C). A lung organoid chip was then developed, and smoke exposure produced similar damage responses to those seen in cell line-derived chips (Figure 8D), confirming model stability. Analysis of key molecules in the organoid model showed transcriptional trends consistent with previous findings, except for KRR1 (Figure 8E). The therapeutic effects of vitamin C and budesonide were validated, showing mitigation of smoke-induced inflammatory gene expression. These results further corroborate our findings using the organoid chip model.

Conclusion

In summary, our study is the first to utilize organ-on-a-chip and organoid technologies, optimizing both the smoke generation process and chip design to create a model that closely replicates contemporary fire-related smoke-induced lung injury. By integrating advanced technologies such as proteomics and computational biology, alongside organoid technology and animal models, we identified potential pathogenic pathways and genes. Simultaneously, various cell types' responses to smoke injury were analyzed at the organ level, and potential therapeutic drugs and combinations were screened. This approach provides a powerful tool for studying the mechanisms and developing treatments for fire-related SI-ALI. However, there are areas for improvement in our study. First, the chip model primarily focuses on early lung injury, neglecting late-stage pathologies such as fibroblast activation and extracellular matrix deposition that may occur following smoke exposure. These factors can contribute to the development of pulmonary fibrosis, significantly impairing respiratory function and affecting patients' quality of life, with currently no effective treatments available. Therefore, future research should delve deeper into the mechanisms of pulmonary fibrosis induced by smoke exposure. Additionally, while the results obtained from the A549 cell line were validated using lung organoids, future studies should consider employing primary lung epithelial cells to more authentically replicate the pathophysiological processes of the lung. Furthermore, the bidirectional flow provided by the perfusion system, along with the absence of neutrophils in the immune cell population, may influence the model's injury responses, warranting further optimization in subsequent research. Lastly, this study did

not incorporate mechanical stretching of the lung. Previous research indicates that respiratory motion can affect the pathophysiological processes of the lung barrier[62], and rapid breathing can lead to shear stress[61] injuries during smoke exposure, potentially exacerbating lung damage. This complexity may complicate the investigation of mechanisms related to smoke-induced toxicity. Consequently, a static model was selected for this study. Future research will build upon these findings to further investigate the mechanisms of smoke-induced lung injury under conditions of respiratory motion.

Table1. Primers information

not-yet-known not-yet-known not-yet-known unknown

human-DOCK2-F	CCCAACAAGCAAACGGTCAT
human-DOCK2-R	CTTGCCGACCCGGACTATTT
human-KRR1-F	ATTCCCACCACCACAACCAG
human-KRR1-R	GCCGCTTCTTCTGATTTGCC
human-TST-F	TTCAAAGCCACACTGGACCG
human-TST-R	GTTGACGGCACCACGGATA
human-RAP1GDS1-F	GCTGTCTGCCCTTATACGACA
human-RAP1GDS1-R	GCCAAAGCAACAAGAGCTTC
human-NIT1-F	GGTAACATCGACGCCAGACA
human-NIT1-R	TGGCAAGCTGGGTGTATTCT
human-COMT-F	CCGCTACCTTCCAGACACAC
human-COMT-R	TTGTCAGCTAGGAGCACCGT
human caspase3-F	GATGTCGATGCAGCAAACCTCA
human caspase3-R	AAACATCACGCATCAATTCCAC
human β-actin F	TGGCACCCAGCACAATGAA
human β-actin R	CTAAGTCATAGTCCGCCTAGAAGCA
human IL-1β-F	GATCACTGAACTGCACGCTCC
human IL-1β-R	CACTTGTTGCTCCATATCCTGT
human IL-6-F	CACTGGCAGAAAACAACCTGA
human IL-6-R	GATTTTCACCAGGCAAGTCTCC
human IL-10-F	AAGCCTTGTCTGAGATGATCCA
human IL-10-R	AAATCGATGACAGCGCCGTA
human NF-ϰB-F	AGATGTTCATAGACAATTTGCCAT
human NF-ϰB-R	CCAAGTCAGATTTCCTCCGAAG
human TNF-α-F	AGGCAGTCAGATCATCTTCTCGAAC
human TNF-α-R	TTATCTCTCAGCTCCACGCCAT

Data availability statement

The combustion components of the materials (Supplementary Text 1), as well as the chip (Supplementary Text 2) and (Supplementary Text 3) proteomics results, can be found in the following dataset: https://data.mendeley.com/datasets/h2gbs2j27v/1.

Acknowledgment

We express our deepest gratitude to Professor Na Li and Professor Yan Zhang from the Department of Anesthesiology at Changhai Hospital for their invaluable guidance in the smoke model and analysis. Special thanks to Dr. Shiqiang Yan from the Second People's Hospital of Shenzhen for his valuable suggestions in constructing the high-throughput lung chips. Lastly, we are immensely grateful to Professor Li Wang from Fudan University for her tremendous support in this project.

Funding sources

This research received support from the Medical Innovation Project of Shanghai Municipal Science and Technology Commission (20Y11900800); Academy for Engineering and Technology of Fudan University (YG2021-025); Shenzhen Science and Technology Program (JCYJ20220530150602006); Naval Medical University Institutional Grant (2023QN063).

Conflicts of interest

The authors declare no competing financial interests or personal relationships that could have been perceived to influence the work reported in this paper.

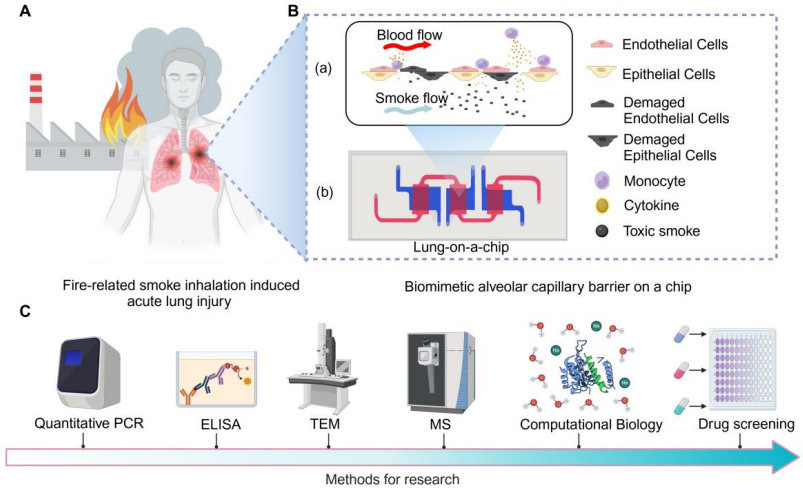

Fig.1. Schematic Diagram of Modeling Fire-Related Smoke inhalation injury using a Human Lung-on-a-chip and Organoid Platform.

In vivo depiction of SI-ALI. **B** . Modeling alveolar capillary barrier on a chip: a. demonstration of the pathological changes in the alveolar-capillary barrier due to smoke inhalation damage in biological systems, b. schematic of the lung chip replicating the aforementioned barrier, with the vascular layer illustrated in red and the alveolar layer in blue. **C** . The relevant techniques used in this study.

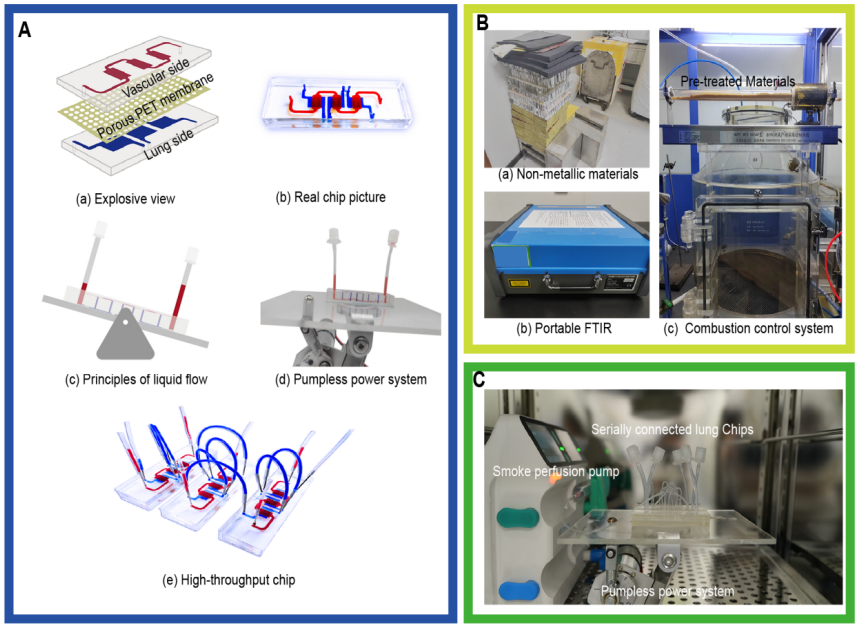

Fig.2. Schematic of the lung-on-a-chip and the pump-less power system, along with the combustion control system.

1. Design of the lung-on-a-chip and the pump-less power system.
2. Combustion control system and smoke detection apparatus: a. non-metallic materials, b. portable Fourier Transform Infrared (FTIR) spectrometer, and c. combustion control system (pre-treated mixed non-metallic materials loaded into the tube furnace).
3. Modeling process of the fire-related smoke-induced acute lung injury based on lung chip model.

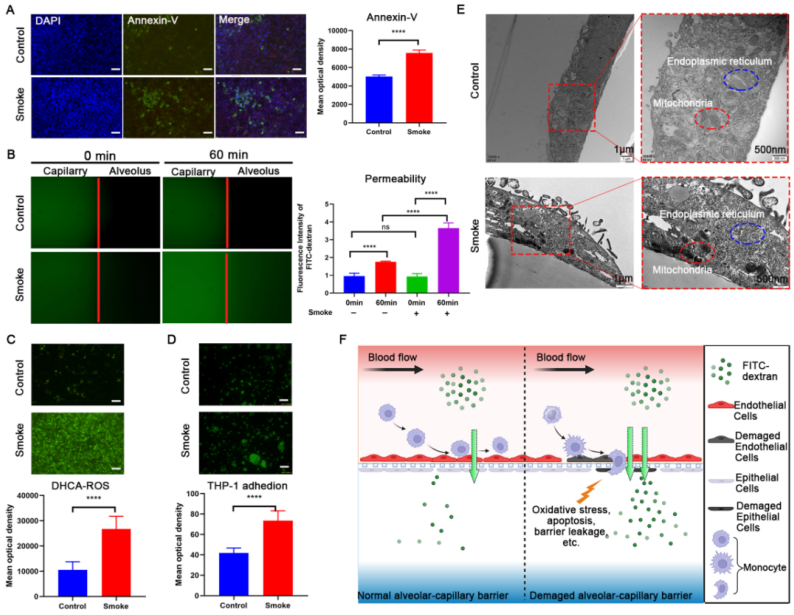

Fig.3. Reproduction of Smoke-Induced Injury on the Chip.

1. Immunofluorescence images depicting apoptosis (Annexin V-FITC stained) across control and smoke-exposed groups, together with a statistical comparison. Data from three independent studies are presented as mean ± standard deviation (SD). n=3, scale bars=30 μm.
2. Detection of FITC-Dextran (40 kDa) translocation from the upper to the lower layer, evidencing alveolar-capillary barrier disruption and quantitative analysis of barrier leakage on the chip by testing fluorescence intensity of FITC-dextran in the alveolar cavity of the chip.it was performed at different time points between the control and smoke-exposed groups (n=6). The results are expressed as mean ± standard deviation (SD).
3. Assessment of oxidative stress (DHCA-ROS stained) on the chip following smoke exposure, accompanied by a corresponding statistical analysis. The results, derived from three independent trials, are expressed as mean ± standard deviation (SD). n=3, scale bars=30 μm.
4. Immunofluorescence imaging to reveal the adhesion patterns of THP-1 cells (Calcein AM and PI stained) in control versus smoke-exposed environments, including an analysis of mean optical density for THP-1 cell adhesion. The results are based on three separate experiments and expressed as mean ± standard deviation (SD). n=3, scale bars, 50 μm.
5. A TEM image representing mitochondrial(red circles) and endoplasmic reticulum(blue circles) in both control and smoke-exposed specimens.
6. Illustration of the pathogenesis of fire-related smoke-induced acute lung injury (SI-ALI), including alveolar-capillary barrier impairment, oxidative stress, apoptosis, and immune cell adhesion.

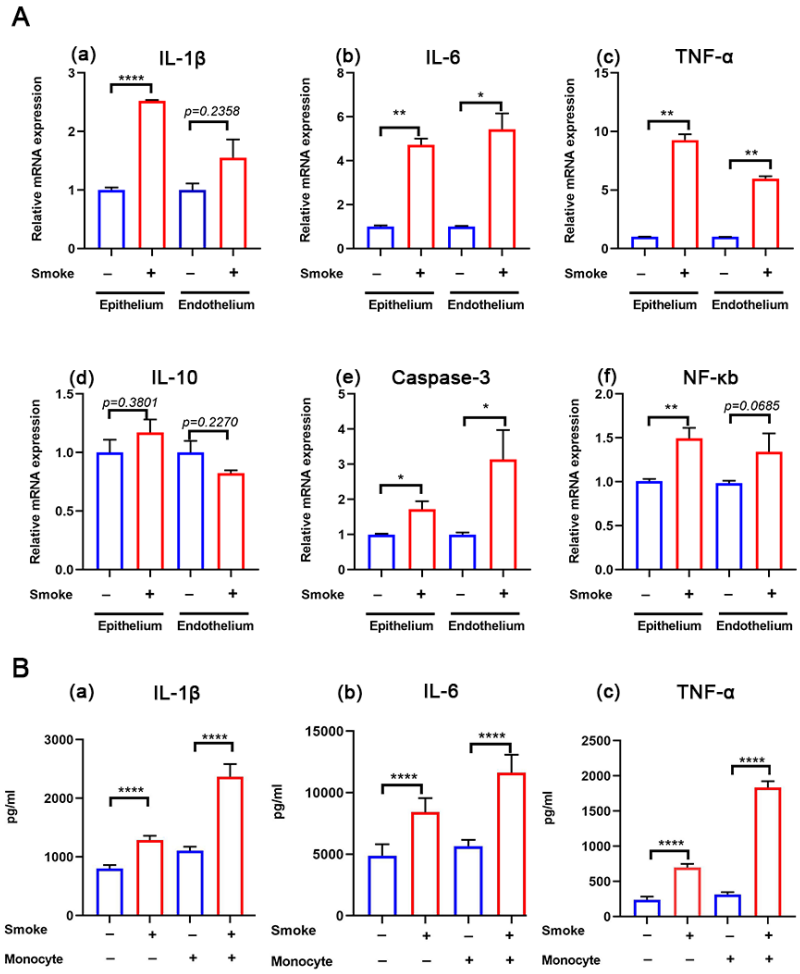

Fig.4. Immune responses associated with smoke-induced lung injury in the chip model.

Comparative expression levels of inflammation and apoptosis-associated genes in the epithelial or endothelial layers of the chip with versus without smoke stimulation were assessed. Three independent assays were conducted on the chip; findings are presented as mean ± standard deviation (SD). n=3.

Quantification of IL-1β, IL-6, and TNF-α secretion from the endothelial layer of the chip after smoke exposure, with or without THP-1 cell interaction. The results are based on three separate experiments and expressed as mean ± standard deviation (SD). n=9.

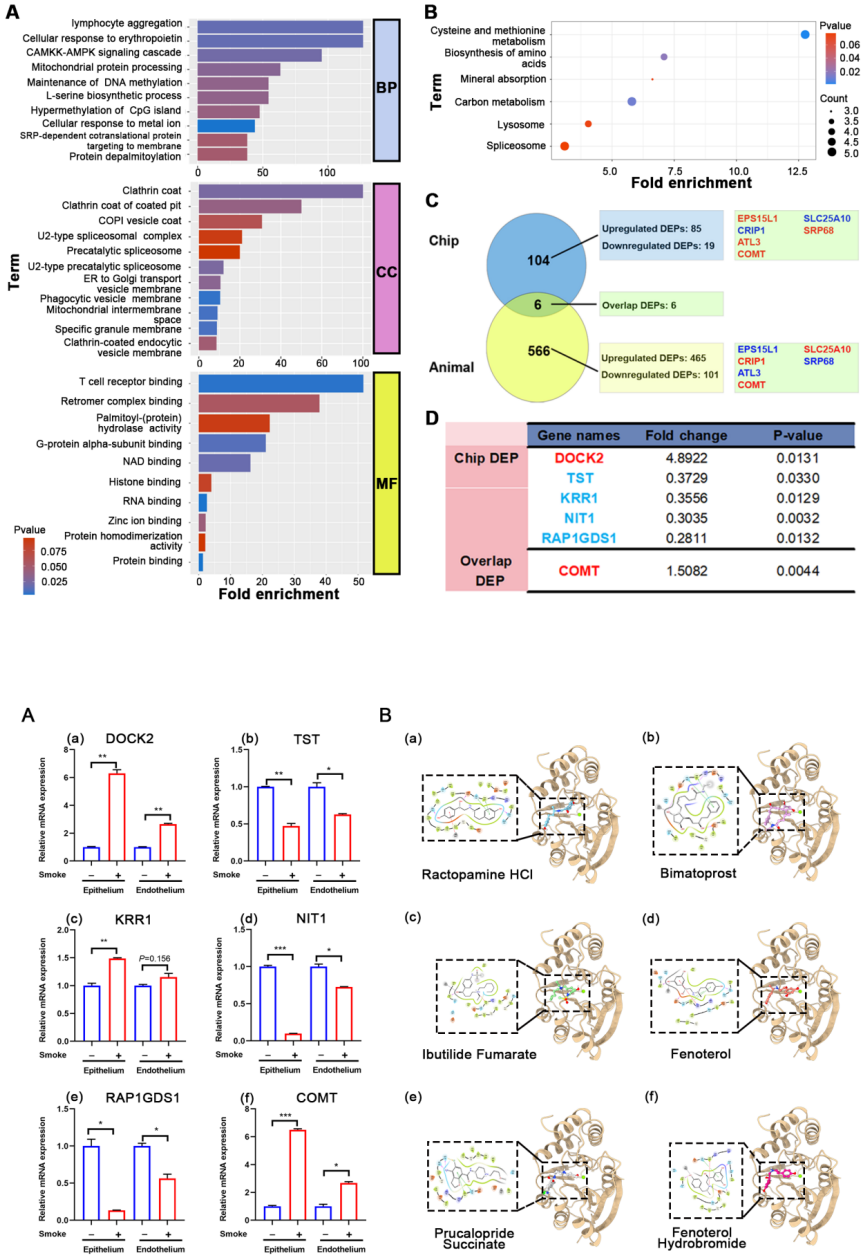

Fig.6. Verification of SI-ALI-associated molecules and molecular docking analysis. Quantitative analysis of mRNA expression levels for the identified representative molecules. Molecular docking results for COMT (Top 6).

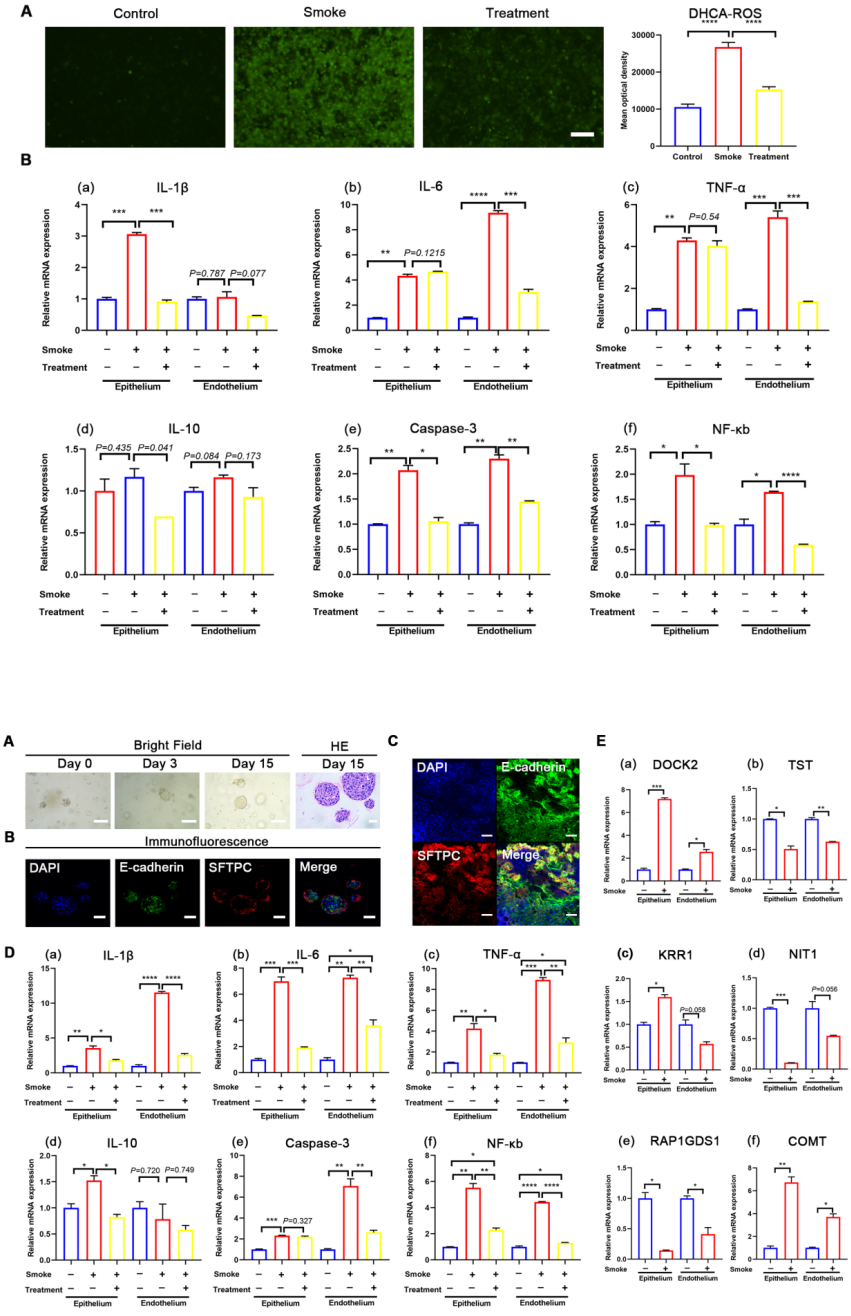

Fig.8. Modeling SI-ALI Using Patient-Derived Lung Organoids and Verification of Genes Associated with SI-ALI.

1. Representative picture of the growth of lung organoid. Scale bars, 50 μm.
2. Representative immunofluorescence images of 3D lung organoid in Matrigel (nuclei stained with DAPI in blue, E-cadherin in green, SFTPC in red). Scale bars, 50 μm.
3. Immunofluorescence micrographs of lung organoid derived epithelial cells on the lung chip (nuclei with DAPI in blue, E-cadherin in green, SFTPC in red). Scale bars, 75 μm.

4. Differential expression of genes involved in inflammation and apoptosis within the epithelial or endothelial layers of the organoid on a chip model , under varying conditions of smoke exposure and treatment. Three separate studies were executed on the chip, with the results expressed as mean ± standard deviation (SD).
5. Quantitative analysis of mRNA expression levels for the identified representative molecules.

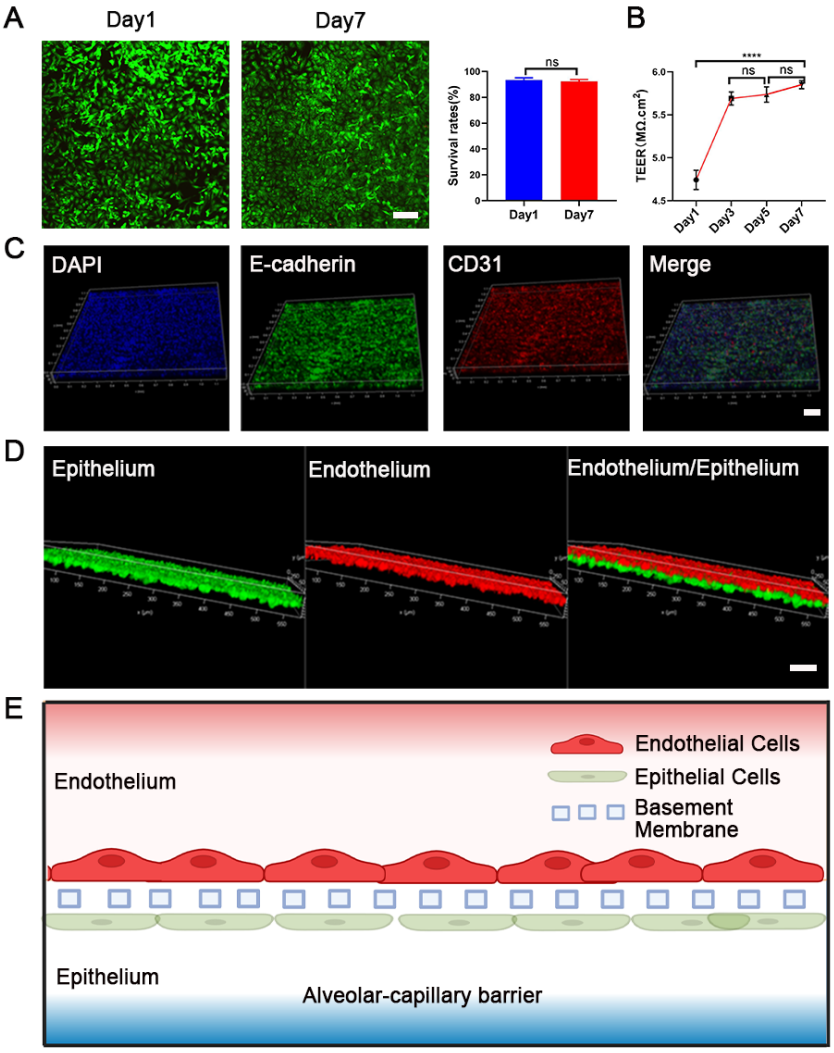

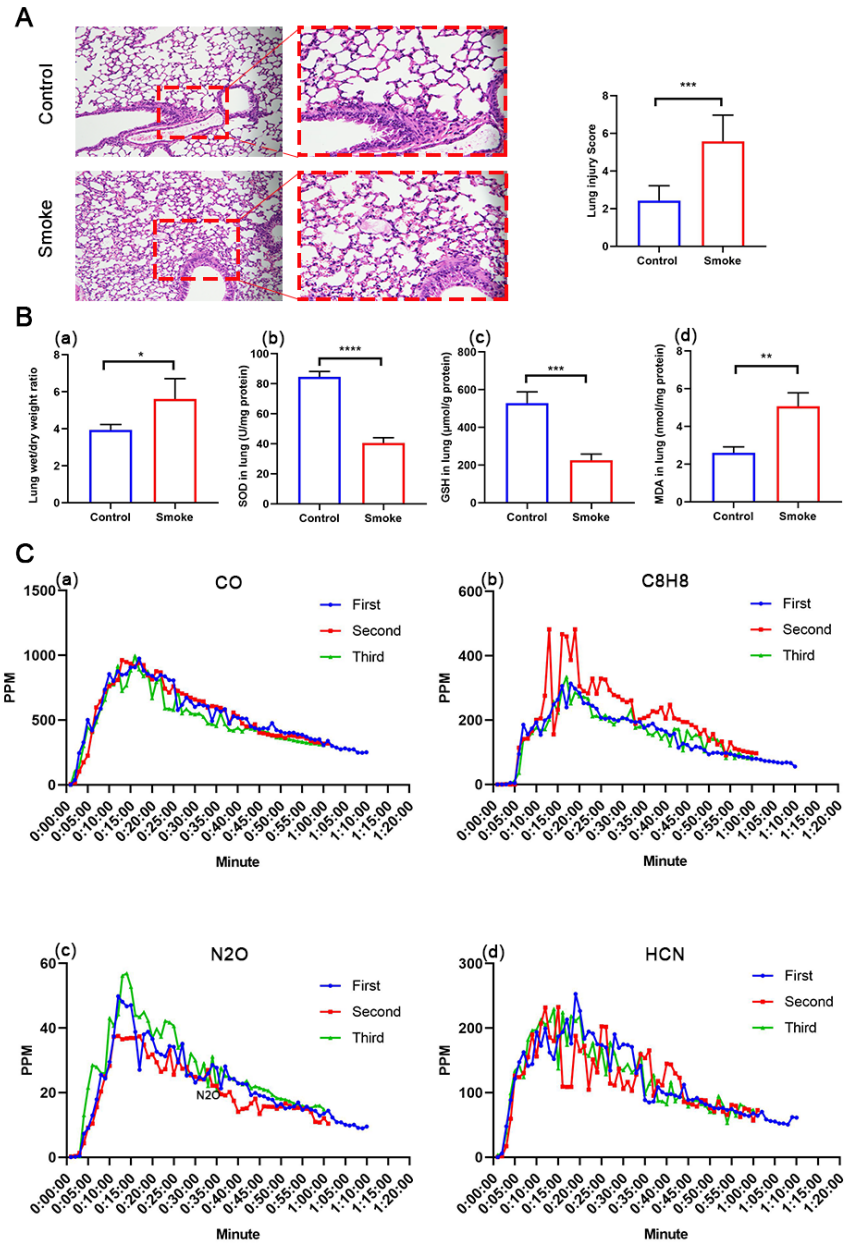

Supplementary Fig.2.

1. Histological evaluation of H&E-stained lung tissue from C57 mice, contrasting control and smoke-exposed groups, complemented by a statistical analysis of lung injury scores (n=6 per group).
2. Lung injury-related indicators: a. lung wet-to-dry ratio, b. superoxide dismutase (SOD), c. glutathione (GSH), and d. malondialdehyde (MDA). Three separate studies were conducted, and the results are expressed as the mean ± standard deviation (SD), n = 8.
3. Variations in the concentration of the main gas components during combustion. Three independent experiments were performed.

KEGG	hsa01200:Carbon metabolism
	hsa03040:Spliceosome
GO-BP	GO:0006614~SRP-dependent cotranslational protein targeting to membrane
	GO:0007264~small GTPase mediated signal transduction
	GO:0000398~mRNA splicing, via spliceosome
	GO:0007030~Golgi organization
	GO:0030036~actin cytoskeleton organization
	GO:0015031~protein transport
GO-CC	GO:0071011~precatalytic spliceosome
	GO:0071005~U2-type precatalytic spliceosome
	GO:0030670~phagocytic vesicle membrane
	GO:0035579~specific granule membrane
	GO:0005681~spliceosomal complex
	GO:0071013~catalytic step 2 spliceosome
	GO:0005884~actin filament
	GO:0042995~cell projection
	GO:0005635~nuclear envelope
	GO:0005925~focal adhesion
	GO:0070062~extracellular exosome
	GO:0005789~endoplasmic reticulum membrane
	GO:0005739~mitochondrion
	GO:0005743~mitochondrial inner membrane
	GO:0005783~endoplasmic reticulum
	GO:0016020~membrane
	GO:0048471~perinuclear region of cytoplasm
	GO:0005794~Golgi apparatus
	GO:0005829~cytosol
	GO:0005654~nucleoplasm
	GO:0005737~cytoplasm
	GO:0005634~nucleus
GO-MF	GO:0003723~RNA binding
	GO:0042803~protein homodimerization activity
	GO:0005515~protein binding

Supplementary Fig.3. Overlap KEGG pathway and GO terms in the lung chip and in vivo mouse model.